AGU ADVANCING EARTH AND SPACE SCIENCES

Geophysical Research Letters

RESEARCH LETTER
10.1029/2024GL109516

Pairwise-Interaction Model Unifies Different Asymptotic Shapes of UHI Intensity

Yunfei Li[1,2], Fabiano L. Ribeiro[3], Bin Zhou[4], and Diego Rybski[2,5]

[1]Potsdam Institute for Climate Impact Research – PIK, Potsdam, Germany, [2]Leibniz Institute of Ecological Urban and Regional Development (IOER), Dresden, Germany, [3]Department of Physics (DFI), Federal University of Lavras (UFLA), Lavras, Brazil, [4]Model-based Environmental Exposure Science, Faculty of Medicine, University of Augsburg, Augsburg, Germany, [5]Complexity Science Hub Vienna, Vienna, Austria

Abstract City size is a primary determinant of the urban heat island (UHI) intensity, with its effects further nuanced by the urban form. But how to factor in the urban form into the UHI assessment remains unresolved. We propose an every-pair-interaction model that meaningfully incorporates urban size and fractal dimension to characterize the UHI intensity. Regression on the summertime surface UHI intensity of 5,000 European cities shows that the model outperforms the simple linear combination of logarithmic size and fractal dimension. Subject to the interplay between the range of the every-pair interaction and the urban fractal shape, the model also represents a generalization as it includes power-law, logarithmic, and saturating size dependence of UHI—all three possibilities have been reported empirically in the literature. Our theoretical framework indicates that the surface UHI intensity saturates with urban size, opening up new research perspectives around UHI intensity.

Plain Language Summary City size is an important determinant of the urban heat island (UHI) intensity. While most studies report a logarithmic dependence of UHI intensity on city size, other functions like power-law and logistic functions have also been reported. In addition, the urban form plays an important role and, intuitively, increased UHI intensity is expected for compact cities. However, how to incorporate urban size and form for modeling UHI is less clear. Based on the perception that every urban site interacts with every other one, whereas the intensity of interaction decreases with the distance, we propose an every-pair-interaction model to characterize the UHI intensity. The model combines urban size and fractal dimension non-linearly and outperforms the simple linear model. It also represents a generalization of the three functional possibilities reported in the literature. Our model indicates that the surface UHI intensity saturates with urban size. Whether the UHI saturates with the expansion of the urban area or follows a continuously increasing trend is relevant for sustainable urban development. Our approach paves the way for fresh research avenues into UHI intensity and urban climate as a whole.

Key Points:

- We propose an every-pair interaction model that unifies urban size and fractal dimension to model surface urban heat island (UHI) intensity
- The model outperforms multi-linear models and is a generalization of three functional shapes of the size dependence of surface UHI intensity
- The empirical results in combination with our theoretical framework indicate that the surface UHI intensity saturates with urban size

Supporting Information:

Supporting Information may be found in the online version of this article.

Correspondence to:

D. Rybski,
ca-dr@rybski.de

Citation:

Li, Y., Ribeiro, F. L., Zhou, B., & Rybski, D. (2024). Pairwise-interaction model unifies different asymptotic shapes of UHI intensity. *Geophysical Research Letters*, *51*, e2024GL109516. https://doi.org/10.1029/2024GL109516

Received 15 APR 2024
Accepted 25 JUL 2024

1. Introduction

Cities cause local warming, resulting in the well-known urban heat island (UHI) effect (Oke et al., 2017). The UHI effect is characterized by enhanced temperature in urban compared to the outlying areas and is attributed mainly to the land surface modification from urbanization (Oke, 1982). Excessive heat associated with the UHI comes with costly impacts on the economy (Estrada et al., 2017) and public health, especially during heat wave events with high risks of heat morbidity and mortality (Gabriel & Endlicher, 2011; Guo et al., 2017; J. Tan et al., 2010; Zhao et al., 2018).

How the UHI is influenced by its main driver, namely urbanization, is a long-standing question (Adolphe, 2001; Chandler, 1964; Chapman et al., 2017; Oke, 1973). Studies on this topic help to better assess the heat risks in view of projected global warming, rapid urbanization, and the growing elderly population (Heaviside et al., 2017). In particular, the influence of urban size and form on the UHI effect is at the center of the research interest (X. Li et al., 2017; Oke, 1973; Stone & Rodgers, 2001; Zhou et al., 2017), since they are among the most important factors involved in the urbanization process.

The primary reasons for the difficulty in quantitatively linking the UHI intensity with urban size are the fluctuations of background climate, and the fact that cities evolve in both structure and size (Chandler, 1964). Despite the challenges, the association between the UHI intensity (ΔT) and the urban size (usually measured by urban area A, population size P, etc.) has been examined quantitatively by studies at different scales, and evidence of

correlations has been reported. The earliest quantitative findings (Ludwig, 1970; Oke, 1973), based on paired urban/rural air temperature observations, report the UHI intensity as a power-law function of urban size measured by population ($\Delta T_a \sim P^{\alpha}$, where $\alpha > 0$ is a constant exponent and the subscript "a" stands for air temperature). Later Oke (1973) finds that the logarithmic function ($\Delta T_a \sim \ln P$) better agrees with the observations than the power-law function. However, the nature of the ground in situ measurements and the UHI definition imply that the effect of urbanization may be underestimated either due to the rural records being affected by urban expansion or due to the urban records failing to capture the effect beyond a certain range. This disadvantage impedes a better understanding of the physical bases of the relationship between ΔT_a and urban size.

The availability of remote sensing data attracts increasing research interest in answering such questions by investigating the *surface* UHI effect of cities. The surface UHI intensity ΔT_s (subscript "s" stands for surface temperature) can be quantified with a spatially explicit land surface temperature (LST) map at the city scale (Peng et al., 2012). Over the years, many studies at different scales statistically confirmed the logarithmic relationship between ΔT_s and the urban size as measured by urban area A (M. Tan & Li, 2015; Zhang et al., 2012; Zhao et al., 2014), that is, $\Delta T_s \sim \ln A$. Some also explored how the background climate controls this relation (Imhoff et al., 2010; X. Li et al., 2017; Y. Li et al., 2021; Manoli et al., 2019). Recently, some studies (e.g., Huang et al., 2019; Zhou et al., 2013) report the surface UHI intensity as a sigmoid function of urban size, given by $\Delta T_s \sim \frac{1}{1+1/f(A)}$, where $f(A)$ is a positive function of the urban area A with $f(A) \to \infty$ for $A \to \infty$. Huang et al. (2019) find that the sigmoid curve better captures the correlations between the surface UHI intensity and urban area than the simple logarithmic function, implying a saturation of ΔT_s for sufficient larger cities. We summarize the empirical findings described above in Table S1 in Supporting Information S1.

In addition to urban size, how cities extend in space (e.g., shape, compact/sprawled) also influences the UHI intensity. It is quite conclusive that the micro-scale urban structure (size, shape, arrangement of urban elements, etc.) affects the thermal environment in the vicinity by determining the fluxes of mass and energy exchange between the urban surface and the atmosphere (Grimmond & Oke, 1999; Martilli, 2014; Yuan et al., 2020). However, these impacts are difficult to describe quantitatively because of a high degree of complexity and extreme morphological heterogeneity at the fine granularity level. Therefore, investigating the mean effects of the interaction between aggregated urban morphology properties and urban climate from a city-scale perspective can help to overcome difficulties resulting from the micro-scale heterogeneity (Adolphe, 2001). A range of geometrical and topological city-scale indicators (e.g., fractal dimension, roundness, area-perimeter ratio, porosity, compactness, contiguity, etc.) have been found statistically correlated with the surface UHI intensity of cities at the regional or global scale (Imhoff et al., 2010; Liang et al., 2020; Liu et al., 2021; Zhou et al., 2017).

Although the UHI intensity is statistically associated with *urban size* and *morphology*, it is still inconclusive how these two factors jointly influence the UHI effect. Previous statistical studies usually end up with linear/multiple-linear models to assess the UHI strength with urban size or urban morphology as predictors (Liang et al., 2020; Liu et al., 2021). However, simple models can hardly capture the interaction between these two factors, since they are likely to function non-linearly—yet the underlying mechanism is to be revealed.

The UHI effect represents a classical complex systems problem. The physical processes at the small scale are well understood. But how they translate into a large-scale measurable, like the UHI intensity, remains challenging because of the emergent characteristics. Previous studies (Y. Li et al., 2020, 2021) have proposed gravitational models to describe the relation between UHI intensity and the location of urban built-up areas. The models are based on the concept of built-up area elements receiving distance-decaying warming effects from other urban elements. This interaction between any pair of built-up area elements of a city diminishes as the distance between them increases, similar to a gravity-based rule. However, the model can only be implemented numerically, and the spatial arrangement of urban built-up areas is not explicitly linked to any quantitative urban form indicators.

Recently, Ribeiro et al. (2024) developed an analytical approximate solution to the every-pair-interaction problem (also known as pairwise-interaction model), following a complex systems approach. The analytical solution is based on the same physical concept as the numerical model, while explicitly integrating the system size and fractal dimension, the latter being a commonly used form indicator. Inspired by this study, we propose to apply the analytical solution to model surface UHI intensity. The proposed model enables us to factor in urban form when characterizing the surface UHI intensity with urban size in a meaningful way. The model shows better statistical performance than multi-linear models based on analyses of the daytime summer surface UHI intensity of 5,000

European cities. Furthermore, exploring the model analytically also enables us to elucidate how urban size and form jointly influence the surface UHI in a complex and non-linear manner. We demonstrate that this model represents a generalization of empirical findings in the literature regarding the relationship between UHI intensity and urban size.

2. Data and Method

We use the binary urban/non-urban Urban Morphological Zones 2006 (UMZ2006) data -set (European Environment Agency, 2010) and apply the City Clustering Algorithm (Rozenfeld et al., 2011) to extract the 5,000 largest urban clusters following the method used in Zhou et al. (2013), Zhou et al. (2017), and Y. Li et al. (2021). UMZ2006 covers 38 European Environmental Agency member states and cooperating countries except Greece, with a spatial resolution of around 250 m.

We chose Europe as the study area because there has been little urban development since the MODIS date became available. The noise introduced by urban growth can be neglected. This allows us to average the LST data from many years for more reliable LST data with less impact from background climate fluctuations and missing values. We extract the multi-annual summer (June, July, and August in 2002–2011) average LST maps from the 8-day composite MODIS LST product (MYD11A2, version 6 (Wan et al., 2015)). We only analyze the LST at around 13:30 local time in this work.

For each of the selected urban clusters, we create a boundary area of approximately the same size as the respective urban cluster. The boundary area excludes other urban cells and cells that have a water surface fraction over 50%. The surface UHI intensity is then calculated as $\Delta T_s = \overline{T}_u - \overline{T}_b$, where $\overline{T}_u$ is the average LST in the urban cluster, and $\overline{T}_b$ is the average LST in the boundary area. The calculation of surface UHI intensity is illustrated in Figure S1 in Supporting Information S1. All temperatures are in °C.

We also extract the fractal dimension D_f of each urban cluster using the box-counting method as described in Zhou et al. (2017). The fractal dimension is a quantitative measure that describes how a geometric pattern fills the space. We use it to analyze the compactness of the urban clusters in the 2-dimensional space, therefore it ranges from 1 to 2. A fractal dimension closer to 1 signifies a linear or strip-like arrangement of urban pixels, while a larger value indicates a more densely packed urban form.

Since the every-pair interaction model is scale-dependent, the estimated parameters of the model are only valid at the corresponding resolution which is bonded with the specific number of urban pixels. For simplicity and consistent comparison of different models, the urban size is given by the cluster size, that is, the number of grid cells N, throughout the manuscript. Given that the spatial area of a single cell is constant, N can be easily converted to the total urban area.

3. Models

This section introduces three models as discussed in the Introduction section.

3.1. Model M1

Inspired by Zhou et al. (2017), we begin with a multi-linear model that combines logarithmic urban size ln N and fractal dimension D_f by

$$\Delta T_s = a \ln N + bD_f + c, \tag{1}$$

where a, b, c are parameters. Please note, in contrast to Zhou et al. (2017), this model does not include the anisometry (a measure of elongation).

3.2. Model M2

The model is grounded in the concept that every urban site (referring to an urban pixel in this work in a narrow sense) interacts with every other, which is also known as the pairwise-interaction model. This interaction could involve the exchange (absorption or discharging) of energy and mass, cool breeze obstruction, or any other physical process. Furthermore, this interaction between locations diminishes in intensity as the distance between

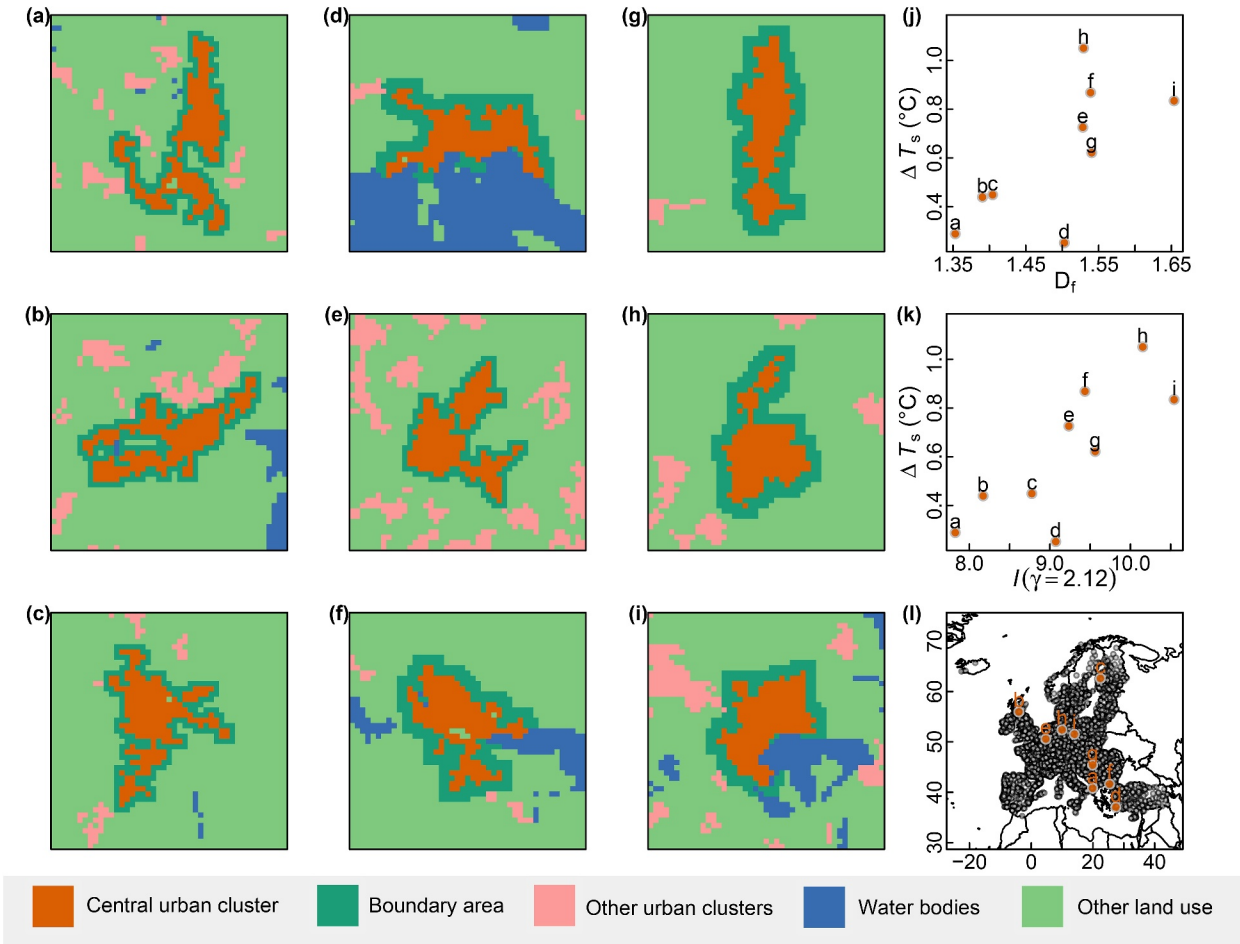

Figure 1. Illustration of the mean interaction field. Panels (a)–(i) show nine examples of urban clusters of 200 cells each, with an ascending order in their corresponding value of I numerically calculated via Equation 2 with $\gamma = 2.12$. (j) Surface urban heat island (UHI) intensity against the fractal dimension for the 9 urban clusters, the labels indicate the respective panels (a)–(i). (k) Surface UHI intensity against the I-values. (l) Locations of the nine examples (orange points). Black points indicate the location of all the urban clusters analyzed in this study.

them increases. This notion was initially introduced in (Y. Li et al., 2020), which proposed an urban morphology indicator to quantify the thermal impact from all built-up areas. This concept was then expanded in the study of surface UHI intensity in European cities (Y. Li et al., 2021). The indicator was found to have a good correlation with the surface UHI intensity.

Here, we explore the quantity I that represents the interaction between urban sites. Given an urban cluster consisting of N grid cells, for a specific cell i, the influence it receives from cell j depends on the distance r_{ij} following $I_{ij} = \frac{1}{r_{ij}^{\gamma}}$, where γ measures how strong the influence decays with the increase of distance. Then the total influence cell i receives from the system is $I_i = \sum_{j \neq i}^{N} \frac{1}{r_{ij}^{\gamma}}$, and on average, the influence received by each cell is

$$I = \frac{1}{N}\sum_{i=1}^{N} I_i = \frac{1}{N}\sum_{i=1}^{N}\sum_{j \neq i}^{N} \frac{1}{r_{ij}^{\gamma}}. \quad (2)$$

Please note that this model is founded on the concept that all physical processes involved in the interaction between sites are modeled by a complex system approach, employing a single and representative parameter (γ). A schematic perspective of this model is presented in Figure S2 in Supporting Information S1.

Since larger clusters consist of more cells and the number of pairs is $N(N-1)/2$, I generally increases with N. Figure 1 shows nine example cities with the same size and different I-values. We can see from Figures 1a–1i that I

can capture the morphology of the urban clusters. Also, Figure 1k demonstrates the clear correlation between I and surface UHI intensity. Thus, we use the quantity I to model the aggregated interactions between all urban cells of a city. We inspect I as a predictor of surface UHI intensity following

$$\Delta T_s = aI(\gamma) + b \quad \text{with} \quad I(\gamma) = \frac{1}{N}\sum_{i=1}^{N}\sum_{j\neq i}^{N}\frac{1}{r_{ij}^{\gamma}}, \tag{3}$$

where a, b, and γ are model parameters.

It has to be noted that this is a quasi-linear model since it cannot be fitted in a conventional way. For each urban cluster, the value I has to be calculated numerically for different γ-values. Here we use equidistant γ-values in the range between 0 and 4 with a step length of 0.01. Then we identify the optimal γ value that leads to the lowest standard residuals σ of the ΔT_s regression.

3.3. Model M3

Recently, an approximate theoretical solution for the quantity I given by Equation 2 was proposed. It strongly agrees with the numerically calculated I-values for various fractal structures (Ribeiro et al., 2024). The analytical value of I is given by

$$I^{\text{theo}} = \frac{N_0 D_f}{(D_f-\gamma)}\left[\left(\frac{N}{N_0}\right)^{1-\frac{\gamma}{D_f}} - r_1^{D_f-\gamma}\right], \tag{4}$$

where N_0 is a parameter, and r_1 is the shortest distance between the neighboring cells of the structure. A summary of its derivation from Equation 2 can be found in Text S1 in Supporting Information S1. For $N \gg N_0$ the analytical solution follows three different curves depending on the difference between γ value and D_f: (a) $\gamma < D_f$, I^{theo} follows a power-law with N; (b) $\gamma > D_f$, saturation of I^{theo} for sufficiently large N; and (c) $\gamma \approx D_f$, $I^{\text{theo}} \sim \ln N$.

In a connected cluster the shortest distance between cells is 1 (there are always grid cells with a common edge), we can use $r_1 = 1$. Thus, we investigate the suitability of I^{theo} as a predictor of surface UHI intensity following

$$\Delta T_s = aI^{\text{theo}} + b, \quad \text{with} \quad I^{\text{theo}} = \frac{N_0 D_f}{(D_f-\gamma)}\left[\left(\frac{N}{N_0}\right)^{1-\frac{\gamma}{D_f}} - 1\right], \tag{5}$$

where a, b, γ, and N_0 are parameters in the regression model to be estimated based on known ΔT_s, N, and D_f. The model is fitted using the non-linear least squares method.

Please note that the difference between the models M2 and M3 is that in M2 the every-pair interactions are calculated numerically, while in M3 an analytical expression for the every-pair interactions is employed. Table 1 gives an overview of the three models. A summary of the relationship and differences between the three models can be found in Text S2 in Supporting Information S1.

4. Results

As shown in Figure 2, the surface UHI intensity is positively correlated with logarithmic urban size ln N and with urban fractal dimension D_f. This is consistent with the work by Zhou et al. (2017). However, in Figure 2a, the small number of large cities makes it difficult to determine the behavior at asymptotic large scales. With increasing urban size, a saturation of the surface UHI intensity, as the sigmoid function proposed by Zhou et al. (2013), is plausible from visual inspection. Statistics based on a much larger sample set of global cities have shown that the sigmoid function agrees better with the association between ΔT_s and urban area than the simple logarithmic function (Huang et al., 2019). Statistically, it is difficult to verify whether there is saturation since the information is carried by the tail of only a few large cities against the bulk of many small ones (Rozenfeld et al., 2011).

The relationship between ΔT_s and D_f as shown in Figure 2b features non-linear statistical properties difficult to infer from the scatter plot. It seems that ΔT_s increases faster with the increase of D_f for cities with larger values of

Table 1
Comparison of the Three Models

Model	M1 $\Delta T_s = a \ln N + bD_f + c$	M2 $\Delta T_s = aI(\gamma) + b$	M3 $\Delta T_s = aI^{\text{theo}}(\gamma, N_0, N, D_f) + b$
Equation	Equation 1	Equation 3	Equation 5
Data	ΔT_s, N, D_f	ΔT_s, $I(\gamma)$	ΔT_s, N, D_f
Parameter estimate (Std. error)	a***: 0.29 (0.09)	a***: 0.28 (0.01)	a***: 0.15 (0.01)
	b***: 2.49 (0.09)	b***: −1.85 (0.05)	b***: −1.77 (0.11)
	c***: −4.55 (0.12)	γ: 2.12	γ***: 2.81 (0.13)
			N_0^{***}: 15.82 (2.53)
σ	0.660	0.635	0.655
AIC	10,029	9,654	9,963
BIC	10,055	9,680	9,996

Note. The equation based on which the model regression is done, the known data, and parameters estimated by the regression, are listed for each of the three models. Please note that model M2 is fitted in a special manner as detailed in Model M2 section. $I(\gamma)$ is calculated based on the spatial information of the clusters so that N and D_f do not appear explicitly. The *** sign indicates $p < 0.001$. The smaller the σ, AIC, and BIC, the better the fitting.

D_f, that is, following a concave curve. However, one needs to bear in mind that D_f for the urban clusters is bounded to $D_f \leq 2$, which can explain the curvature for cities with larger fractal dimensions.

We compare the statistics of the three models in terms of the residual standard error σ, the Akaike information criterion (AIC), and Bayesian information criterion (BIC). We refer to (Kuha, 2004) for details about these two information criteria. As listed in Table 1 (together with the estimated parameters), the relative performances of the three models are consistent across the chosen criteria. Model M2 outperforms the other two regarding standard residual, AIC, and BIC. Although having one additional parameter, model M3 performs better than model M1 as shown by AIC and BIC which favor simpler models with fewer parameters.

Model M2's superior performance is attributed to its consideration of microscopic details, whereas M3 is derived from an approximate solution (detailed in Text S1 in Supporting Information S1). However, model M3 offers an advantage since, for common use cases, the computational demands of model M2 are excessive. For instance, the double-sum in Equation 3 implies a computational complexity of $O(N^2)$ for each γ-value. Moreover, model M3 facilitates an understanding that would not be achievable through model M2 alone. It interprets the complexity of

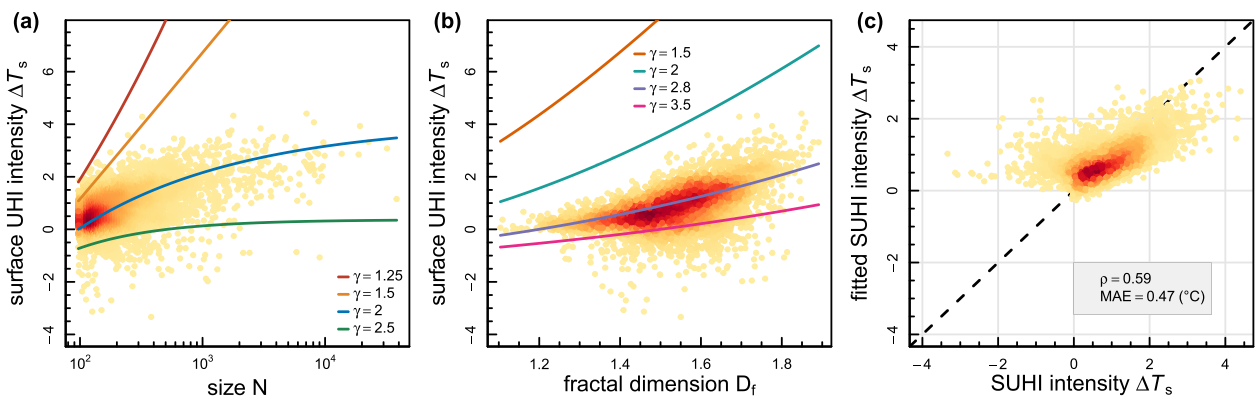

Figure 2. Surface urban heat island (UHI) intensity and urban size or fractal dimension. The color of the points indicates the point density (red: high). (a) The UHI intensity is plotted as a function of urban size N. The solid curves follow Equation 5 (model M3) with $N_0 = 15.82$, $a = 0.15$, $b = -1.77$, and $D_f = 1.5$, with different colors corresponding to γ values of 1.25, 1.5, 2, and 2.5, respectively. (b) The UHI intensity is plotted as a function of the fractal dimension for the same set of cities. The solid curves follow Equation 5 with $N_0 = 15.82$, $a = 0.15$, $b = -1.77$, and $N = 1{,}000$, with different colors corresponding to γ values of 1.5, 2, 2.8, and 4, respectively. (c) Visualization of the performance of model M3. Fitted (with Equation 5) surface UHI intensities are plotted versus the measured values (in °C). The Pearson's correlation coefficient between the predicted and the measured values is 0.59, and the prediction's mean absolute error is 0.47°C. The dashed black line corresponds to the ideal diagonal. The estimated values of the parameters as listed in Table 1 are used. Corresponding results for the other two models look very similar.

the spatial arrangement of the urban sites by a small set of macroscopic parameters, namely N_0 and D_f, and how they relate to the interaction parameter γ.

In both models, M2 and M3, we obtain $\gamma > 2$, that is, $\gamma > D_f$ for all cities. This indicates a short-range regime (Campa & Dauxois, 2014; Campa et al., 2009; Ribeiro et al., 2024), that is, the interactions decrease strongly with the distance so that no amplifying effect occurs due to the urban agglomeration. This means, according to the properties of M3 discussed in Section 3.3, the surface UHI intensity saturates with city size. It is remarkable that Zhou et al. (2013) and Huang et al. (2019) also found saturation for *surface* UHI. The fact that the γ estimates of both models differ can be attributed to the non-linear character of the models.

In Figure 2c the fitted surface UHI intensities are plotted against the observed ones. We can see that model M3 reproduces the surface UHI intensity of most cities with fair accuracy. However, the ability of model M3 to reproduce the surface UHI intensities on both extreme ends is rather limited. Actually, all three models have similar performance in reproducing the extreme UHI intensities. The reason is that the UHI effect of a city is also strongly influenced by its background environment (Lai et al., 2021; X. Li et al., 2017) which is not considered in this study. Y. Li et al. (2021) have demonstrated that cities with very low and very high surface UHI intensities are often situated in distinct environmental settings, such as valleys, coastal stretches, or near water bodies. They also showed that extreme values can be reproduced much better when considering both background climate factors and topographical conditions.

Following the analyses by Ribeiro et al. (2024), we illustrate in Figure 2a that model M3 represents a generalization of different UHI intensity versus urban size relations found in previous studies. We take $D_f = 1.5$ as an example since in our data the majority of the cities have a fractal dimension around this value. Equation 5 can take different shapes depending on the value of γ. When $\gamma < D_f$, the curve follows the power-law, that is, $I^{\text{theo}} \sim N^{1-\frac{\gamma}{D_f}}$; when $\gamma \simeq D_f$, the curve is logarithmic, that is, $\Delta T_s \sim \ln N$; when $\gamma > D_f$, a saturation of the curve will appear, see Figure 2a. The exponent of the power-law relation $\left(1 - \frac{\gamma}{D_f}\right)$ suggests that when D_f approaches γ, the size dependence of $\Delta T(N)$ becomes statistically indistinguishable from the logarithmic shape since the exponent approaches zero. Previous studies that describe the scale dependence of UHI intensity with power-law functions also report very small values of the exponent (D. Li & Wang, 2019; Oke, 1973). In Figure 2b we show example curves of Equation 5 for constant size but variable fractal dimension. The curvature with $\gamma = 2.8$ generally describes the trend of the point cloud, which supports the every-pair-interaction model. To illustrate how Equation 5 behaves depending on the γ values, in Figures S2a–S2b in Supporting Information S1, we show some example curves of it with extended ranges of city size and fractal dimension.

5. Discussion

Model M1 lacks any motivation except that a linear combination of independent variables is the first thing to experiment with. In contrast, the urban morphology quantity I in Equation 2 on which model M2 is based, is motivated in a meaningful way since it aggregates (a) the interaction effect between any pair of the urban sites and (b) the spatial arrangement of these sites.

The theoretical solution I^{theo} in model M3 shares the same motivation as in model M2. In addition, it includes the fractal dimension of urban clusters, which has been found to be an effective factor in linking urban compactness with the surface UHI intensity. Moreover, as urban compactness indicators, both every-pair-interaction quantity I and fractal dimension are special since the spatial arrangement of every individual urban site affects the measure. In other words, they represent ideal indicators to characterize the city-scale urban morphology and to link the urban morphology with the UHI effect aggregated to the city scale. We can consider M2 as a microscopic model because it encompasses all the intricacies of the spatial distribution of the sites. M3, which is the analytical approximate solution of the double sum used in M2, can be seen as a macroscopic model, as it captures not the details but the essence of the phenomenon.

We would like to emphasize that analyzing the data without a theory is not possible to infer if there is a saturation or not in ΔT with the city size. However, the model proposed here, which has physical interpretation and justification, suggests a saturation for the considered *surface* UHI. It is because the estimated every-pair-interaction range is larger than the fractal dimension ($\gamma > D_f$), and, according to model M3, such values imply saturation. More specifically, according to the results, the interaction between urbanized cells (e.g., in the form of

heat exchange) behaves in a short-range regime. In other words, saturation happens because the interaction range between urban cells has a typical and short length.

Despite the statistical evidence on the correlation of the UHI intensity with urban size and urban morphology, the physical mechanism behind the relation is not clear. Without guidance from a comprehensive understanding of the physical basis, it is challenging to come up with models that quantitatively describe the response of UHI intensity to urban size and morphology in a meaningful way. Interestingly, the every-pair-interaction model represents a generalization as it includes power-law, logarithmic, and saturating urban size dependence of the UHI intensity—all three shapes have been reported empirically in the literature (see Table S1 in Supporting Information S1). The actual shape depends on the values of γ and D_f (Ribeiro et al., 2024).

Our work opens a range of perspectives for future research. In the case of $\gamma < 2$ we also expect a transition between long- and short-range interactions. This is because of correlations between city size and fractal dimension (larger cities are more compact and exhibit larger D_f, see Figure S4 in Supporting Information S1). We obtain a Pearson correlation coefficient reaching 0.58 between ln N and D_f in our data. Thus, for $\gamma < 2$ the typical fractal dimension can potentially trespass the γ-value with increasing city size, implying a transition from short-range ($D_f < \gamma$) to long-range ($D_f > \gamma$) interactions. Consequently, we would expect a critical city size $N_\times$ at which a transition occurs toward power-law behavior for large cities. Nevertheless, the analytical model suggests that less compact development is always favorable for its smaller increment of the UHI intensity per unit of urban growth.

It would be intriguing to apply the every-pair-interactions model to the canopy UHI effect since the air temperature is more relevant to the thermal comfort of the population. Would such an analysis also lead to $\gamma > 2$, implying saturation of canopy UHI with city size, or would it result in $\gamma \leq 2$, ruling out the saturation? Whether or not ΔT saturates is crucial in light of ongoing urbanization and climate change. In particular, in the global south where urbanization leads to ever-growing cities. Climate change adds to this trend and considerable heat burden needs to be anticipated in many regions. Accordingly, whether or not the UHI intensity saturates along ongoing urbanization, can make a big difference in the livability of the largest cities.

It remains to understand what the exponent γ represents. In the radiation sense, we expect $\gamma = 2$ because the surface of a sphere goes as $\sim r^2$ with the radius r. In the case of 2 dimensions, we would expect $\gamma = 1$, that is, the length (perimeter) of a circle goes as $\sim r$. Diffusion in terms of Brownian motion goes as $\sim r^{1/2}$ (root-mean-square displacement according to Fick's law). Thus, the γ-exponent can characterize the physical processes (or their combination) behind the interactions.

Before we discuss that the γ-exponents relate to the physical processes behind the interactions, it is fair to assume that also the background climate plays an important role in determining the γ-value. Therefore, the γ value provides the interface where the climatic factors can be introduced. Accordingly, a systematic study of the influence of the background climate would be desirable. Such an analysis could for example, repeat our work by separating a bigger sample by climate zones. One could also perform a complementary analysis to (Y. Li et al., 2020) and vary the climate while keeping the city structure constant. Ultimately, an ambitious goal of a holistic quantitative tool for UHI assessment might be achieved.

Since Equation 2 is the theoretical expression applying only on 2D planar surface (Ribeiro et al., 2024), in this work we do not consider the density of the urban sites (e.g., sealed surface fraction, building height, floor area ratio, etc.). It has been shown in previous work (Y. Li et al., 2020, 2021) that the metrics as a proxy of urban density can improve the predictive power of the numerically calculated quantity I. Some other limitations of this work are discussed in Text S3 in Supporting Information S1.

6. Conclusion

In summary, we propose an every-pair-interaction model to characterize the UHI intensity based on city size and fractal dimension in a meaningful way. The model combines urban size and fractal dimension non-linearly and outperforms the simple linear model. The every-pair interaction model also represents a generalization of the three functional possibilities reported in the literature. Our model indicates that the surface UHI intensity saturates with urban size. Since the question of whether the UHI saturates with the expansion of the urban area is highly relevant for sustainable urban development, our approach paves the way for fresh research avenues into UHI intensity and urban climate as a whole.

Data Availability Statement

The Urban Morphological Zones 2006 data (European Environment Agency, 2010) and 8-day composite MODIS LST data (MYD11A2, version 6, Wan et al., 2015) are publicly accessible from the providers. The processed data set that supports this work, is shared at Y. Li (2024).

Acknowledgments
Y. Li and D. Rybski would like to thank the German Research Foundation (DFG) for financial support (Urban Percolations project; 451083179). D. Rybski also appreciates financial support from Leibniz Association (project CriticaL). F. L. Ribeiro thanks CNPq (Grants 403139/2021-0 and 424686/2021-0) and Fapemig (Grant APQ-00829-21) for financial support. Open Access funding enabled and organized by Projekt DEAL.

References

Adolphe, L. (2001). A simplified model of urban morphology: Application to an analysis of the environmental performance of cities. *Environment and Planning B*, *28*(2), 183–200. https://doi.org/10.1068/b2631

Campa, A., & Dauxois, T. (2014). *Physics of long-range interacting systems*. Oxford University Press. https://doi.org/10.1093/acprof:oso/9780199581931.001.0001

Campa, A., Dauxois, T., & Ruffo, S. (2009). Statistical mechanics and dynamics of solvable models with long-range interactions. *Physics Reports*, *480*(3–6), 57–159. https://doi.org/10.1016/j.physrep.2009.07.001

Chandler, T. (1964). City growth and urban climates. *Weather*, *19*(6), 170–171. https://doi.org/10.1002/j.1477-8696.1964.tb02116.x

Chapman, S., Watson, J. E. M., Salazar, A., Thatcher, M., & McAlpine, C. A. (2017). The impact of urbanization and climate change on urban temperatures: A systematic review. *Landscape Ecology*, *32*(10), 1921–1935. https://doi.org/10.1007/s10980-017-0561-4

Estrada, F., Botzen, W. W., & Tol, R. S. (2017). A global economic assessment of city policies to reduce climate change impacts. *Nature Climate Change*, *7*(6), 403–406. https://doi.org/10.1038/nclimate3301

European Environment Agency. (2010). Urban morphological zones 2006. [dataset]. Barcelona. https://sdi.eea.europa.eu/data/8ab00854-d08f-43b1-b78f-447ce13857d1

Gabriel, K. M., & Endlicher, W. R. (2011). Urban and rural mortality rates during heat waves in Berlin and Brandenburg, Germany. *Environmental Pollution*, *159*(8–9), 2044–2050. https://doi.org/10.1016/j.envpol.2011.01.016

Grimmond, C. S. B., & Oke, T. R. (1999). Aerodynamic properties of urban areas derived from analysis of surface form. *Journal of Applied Meteorology and Climatology*, *38*(9), 1262–1292. https://doi.org/10.1175/1520-0450(1999)038<1262:APOUAD>2.0.CO;2

Guo, Y., Gasparrini, A., Armstrong, B. G., Tawatsupa, B., Tobias, A., Lavigne, E., et al. (2017). Heat wave and mortality: A multicountry, multicommunity study. *Environmental Health Perspectives*, *125*(8), 087006. https://doi.org/10.1289/EHP1026

Heaviside, C., Macintyre, H., & Vardoulakis, S. (2017). The urban heat island: Implications for health in a changing environment. *Current Environmental Health Reports*, *4*(3), 296–305. https://doi.org/10.1007/s40572-017-0150-3

Huang, K., Li, X., Liu, X., & Seto, K. C. (2019). Projecting global urban land expansion and heat island intensification through 2050. *Environmental Research Letters*, *14*(11), 114037. https://doi.org/10.1088/1748-9326/ab4b71

Imhoff, M. L., Zhang, P., Wolfe, R. E., & Bounoua, L. (2010). Remote sensing of the urban heat island effect across biomes in the continental USA. *Remote Sensing of Environment*, *114*(3), 504–513. https://doi.org/10.1016/j.rse.2009.10.008

Kuha, J. (2004). Aic and bic: Comparisons of assumptions and performance. *Sociological Methods & Research*, *33*(2), 188–229. https://doi.org/10.1177/0049124103262065

Lai, J., Zhan, W., Quan, J., Liu, Z., Li, L., Huang, F., et al. (2021). Reconciling debates on the controls on surface urban heat island intensity: Effects of scale and sampling. *Geophysical Research Letters*, *48*(19), e2021GL094485. https://doi.org/10.1029/2021GL094485

Li, D., & Wang, L. (2019). Sensitivity of surface temperature to land use and land cover change-induced biophysical changes: The scale issue. *Geophysical Research Letters*, *46*(16), 9678–9689. https://doi.org/10.1029/2019GL084861

Li, X., Zhou, Y., Asrar, G. R., Imhoff, M., & Li, X. (2017). The surface urban heat island response to urban expansion: A panel analysis for the conterminous United States. *Science of the Total Environment*, *605*, 426–435. https://doi.org/10.1016/j.scitotenv.2017.06.229

Li, Y. (2024). Data of surface UHI, urban size, and fractal dimension [dataset]. https://doi.org/10.6084/m9.figshare.25592451

Li, Y., Schubert, S., Kropp, J. P., & Rybski, D. (2020). On the influence of density and morphology on the urban heat island intensity. *Nature Communications*, *11*(1), 2647. https://doi.org/10.1038/s41467-020-16461-9

Li, Y., Zhou, B., Glockmann, M., Kropp, J. P., & Rybski, D. (2021). Context sensitivity of surface urban heat island at the local and regional scales. *Sustainable Cities and Society*, *74*, 103146. https://doi.org/10.1016/j.scs.2021.103146

Liang, Z., Wang, Y., Huang, J., Wei, F., Wu, S., Shen, J., et al. (2020). Seasonal and diurnal variations in the relationships between urban form and the urban heat island effect. *Energies*, *13*(22), 5909. https://doi.org/10.3390/en13225909

Liu, H., Huang, B., Zhan, Q., Gao, S., Li, R., & Fan, Z. (2021). The influence of urban form on surface urban heat island and its planning implications: Evidence from 1288 urban clusters in China. *Sustainable Cities and Society*, *71*, 102987. https://doi.org/10.1016/j.scs.2021.102987

Ludwig, F. (1970). Urban air temperatures and their relation to extraurban meteorological measurements. *American Society of Heating, Refrigerating and Air-Conditioning Engineers*, *70*, 9–40.

Manoli, G., Fatichi, S., Schläpfer, M., Yu, K., Crowther, T. W., Meili, N., et al. (2019). Magnitude of urban heat islands largely explained by climate and population. *Nature*, *573*(7772), 55–60. https://doi.org/10.1038/s41586-019-1512-9

Martilli, A. (2014). An idealized study of city structure, urban climate, energy consumption, and air quality. *Urban Climate*, *10*, 430–446. https://doi.org/10.1016/j.uclim.2014.03.003

Oke, T. R. (1973). City size and the urban heat island. *Atmospheric Environment*, *7*(8), 769–779. https://doi.org/10.1016/0004-6981(73)90140-6

Oke, T. R. (1982). The energetic basis of the urban heat island. *Quarterly Journal of the Royal Meteorological Society*, *108*(455), 1–24. https://doi.org/10.1002/qj.49710845502

Oke, T. R., Mills, G., Christen, A., & Voogt, J. A. (2017). *Urban climates*. Cambridge University Press. https://doi.org/10.1017/9781139016476

Peng, S., Piao, S., Ciais, P., Friedlingstein, P., Ottle, C., Bréon, F.-M., et al. (2012). Surface urban heat island across 419 global big cities. *Environmental Science & Technology*, *46*(2), 696–703. https://doi.org/10.1021/es2030438

Ribeiro, F. L., Li, Y., Born, S., & Rybski, D. (2024). Analytical solution for the long- and short-range every-pair-interactions system. *Chaos, Solitons & Fractals*, *183*, 114771. https://doi.org/10.1016/j.chaos.2024.114771

Rozenfeld, H. D., Rybski, D., Gabaix, X., & Makse, H. A. (2011). The area and population of cities: New insights from a different perspective on cities. *The American Economic Review*, *101*(5), 2205–2225. https://doi.org/10.1257/aer.101.5.2205

Stone, B., & Rodgers, M. O. (2001). Urban form and thermal efficiency: How the design of cities influences the urban heat island effect. *Journal of the American Planning Association*, *67*(2), 186–198. https://doi.org/10.1080/01944360108976228

Tan, J., Zheng, Y., Tang, X., Guo, C., Li, L., Song, G., et al. (2010). The urban heat island and its impact on heat waves and human health in Shanghai. *International Journal of Biometeorology*, *54*(1), 75–84. https://doi.org/10.1007/s00484-009-0256-x

Tan, M., & Li, X. (2015). Quantifying the effects of settlement size on urban heat islands in fairly uniform geographic areas. *Habitat International*, *49*, 100–106. https://doi.org/10.1016/j.habitatint.2015.05.013

Wan, Z., Hook, S., & Hulley, G. (2015). Mod11a2 modis/terra land surface temperature/emissivity 8-day l3 global 1km sin grid v006 [dataset]. *NASA EOSDIS Land Processes DAAC*. https://doi.org/10.5067/MODIS/MYD11A2.006

Yuan, C., Adelia, A. S., Mei, S., He, W., Li, X.-X., & Norford, L. (2020). Mitigating intensity of urban heat island by better understanding on urban morphology and anthropogenic heat dispersion. *Building and Environment*, *176*, 106876. https://doi.org/10.1016/j.buildenv.2020.106876

Zhang, P., Imhoff, M. L., Bounoua, L., & Wolfe, R. E. (2012). Exploring the influence of impervious surface density and shape on urban heat islands in the northeast United States using MODIS and landsat. *Canadian Journal of Remote Sensing*, *38*(4), 441–451. Retrieved from https://www.tandfonline.com/doi/full/10.5589/m12-036?scroll=top&needAccess=true

Zhao, L., Lee, X., Smith, R. B., & Oleson, K. (2014). Strong contributions of local background climate to urban heat islands. *Nature*, *511*(7508), 216–219. https://doi.org/10.1038/nature13462

Zhao, L., Oppenheimer, M., Zhu, Q., Baldwin, J. W., Ebi, K. L., Bou-Zeid, E., et al. (2018). Interactions between urban heat islands and heat waves. *Environmental Research Letters*, *13*(3), 034003. https://doi.org/10.1088/1748-9326/aa9f73

Zhou, B., Rybski, D., & Kropp, J. P. (2013). On the statistics of urban heat island intensity. *Geophysical Research Letters*, *40*(20), 5486–5491. https://doi.org/10.1002/2013GL057320

Zhou, B., Rybski, D., & Kropp, J. P. (2017). The role of city size and urban form in the surface urban heat island. *Scientific Reports*, *7*(1), 4791. https://doi.org/10.1038/s41598-017-04242-2